Biochimica et Biophysica Acta 1848 (2015) 1481–1489

Contents lists available at ScienceDirect

Biochimica et Biophysica Acta

journal homepage: www.elsevier.com/locate/bbamem

Membrane targeting of the yeast exocyst complex

Roman Pleskot [a,b,*], Lukasz Cwiklik [b,c], Pavel Jungwirth [b,d], Viktor Žárský [a,e], Martin Potocký [a,*]

[a] Institute of Experimental Botany, Academy of Sciences of the Czech Republic, 165 02 Prague, Czech Republic
[b] Institute of Organic Chemistry and Biochemistry, Academy of Sciences of the Czech Republic, 166 10 Prague, Czech Republic
[c] J. Heyrovsky Institute of Physical Chemistry, Academy of Sciences of the Czech Republic, 182 23 Prague, Czech Republic
[d] Department of Physics, Tampere University of Technology, FI-33101 Tampere, Finland
[e] Department of Experimental Plant Biology, Charles University in Prague, 128 44 Prague, Czech Republic

ARTICLE INFO

Article history:
Received 21 January 2015
Received in revised form 20 March 2015
Accepted 24 March 2015
Available online 30 March 2015

Keywords:
The exocyst complex
Exo70p
Sec3p
Rho1p
Phosphatidylinositol (4,5)-bisphosphate
Molecular dynamics simulation

ABSTRACT

The exocytosis is a process of fusion of secretory vesicles with plasma membrane, which plays a prominent role in many crucial cellular processes, e.g. secretion of neurotransmitters, cytokinesis or yeast budding. Prior to the SNARE-mediated fusion, the initial contact of secretory vesicle with the target membrane is mediated by an evolutionary conserved vesicle tethering protein complex, the exocyst. In all eukaryotic cells, the exocyst is composed of eight subunits — Sec5, Sec6, Sec8, Sec10, Sec15, Exo84 and two membrane-targeting landmark subunits Sec3 and Exo70, which have been described to directly interact with phosphatidylinositol (4,5)-bisphosphate (PIP_2) of the plasma membrane. In this work, we utilized coarse-grained molecular dynamics simulations to elucidate structural details of the interaction of yeast Sec3p and Exo70p with lipid bilayers containing PIP_2. We found that PIP_2 is coordinated by the positively charged pocket of N-terminal part of Sec3p, which folds into unique Pleckstrin homology domain. Conversely, Exo70p interacts with the lipid bilayer by several binding sites distributed along the structure of this exocyst subunit. Moreover, we observed that the interaction of Exo70p with the membrane causes clustering of PIP_2 in the adjacent leaflet. We further revealed that PIP_2 is required for the correct positioning of small GTPase Rho1p, a direct Sec3p interactor, prior to the formation of the functional Rho1p-exocyst-membrane assembly. Our results show the critical importance of the plasma membrane pool of PIP_2 for the exocyst function and suggest that specific interaction with acidic phospholipids represents an ancestral mechanism for the exocyst regulation.

© 2015 Elsevier B.V. All rights reserved.

1. Introduction

All eukaryotic cells display some aspects of polar organization, which, in essence, is achieved by the asymmetric localization of intracellular structures and components. This phenomenon has been described to play a critical role in the development of neuronal cells, in the growth of fungal hyphae or plant pollen tubes and root hairs [1–3]. The cell polarity is mediated by the asymmetric distribution of proteins and lipids in the specialized domains in the plasma membrane (PM). The polar domains are formed by properly balanced exocytosis, endocytosis and two-dimensional lateral mobility within PM [4]. Exocytosis is a process of the fusion of secretory vesicles with PM. Secretory vesicles, that bud from the trans-Golgi network or recycling endosome, are transported along cytoskeletal networks to their destination, where they are tethered and finally fused with PM. The tethering step, described as the initial contact of the secretory vesicle with the target PM prior to the SNARE-catalyzed membrane fusion [5], is in many cases mediated by the evolutionary conserved multiprotein complex, the exocyst. All subunits of the exocyst were discovered in the budding yeast by genetic screens for mutants in secretion [6] and the budding yeast has been an invaluable model in identifying basic principles of the exocyst functions. In addition to its mechanistic role in tethering, the exocyst also determines the region of PM, where exocytosis takes place. The exocyst is composed of eight subunits, Sec3, Sec5, Sec6, Sec8, Sec10, Sec15, Exo70, and Exo84. The whole exocyst complex has the molecular weight of approximately 750 kDa with subunits ranging in size from 70 to 150 kDa [7]. The exocyst is a member of the structurally and functionally related Complex Associated with Tethering Containing Helical Rods (CATCHR) family, which also contains COG, Dsl and GARP complexes, that tether vesicles at the Golgi, ER and endosomes, respectively [8]. Several recent studies have provided valuable insights into the structural organization of the exocyst complex [9]. So far, partial crystal structures of five exocyst components have been obtained. These include near full-length of yeast Exo70 (Exo70p, Fig. 1), the C-terminal part of Exo84p and Sec6p, and the N-terminal part of Sec3p [10–14]. In addition, the crystal structures of the near full-length mouse Exo70, the C-terminal part of Drosophila Sec15 and the Ral-binding domain of rat Exo84 were solved [15]. Yeast Exo70p (amino acid residues 67–623) folds into an elongated rod that is 160 Å long and 30–35 Å wide, it comprises nineteen α-helices and

* Corresponding authors at: Institute of Experimental Botany, v. v. i., Academy of Sciences of the Czech Republic, Rozvojova 263, Prague 6, 165 02, Czech Republic. Tel.: +420 225106457.
E-mail addresses: pleskot@ueb.cas.cz (R. Pleskot), potocky@ueb.cas.cz (M. Potocký).

http://dx.doi.org/10.1016/j.bbamem.2015.03.026
0005-2736/© 2015 Elsevier B.V. All rights reserved.

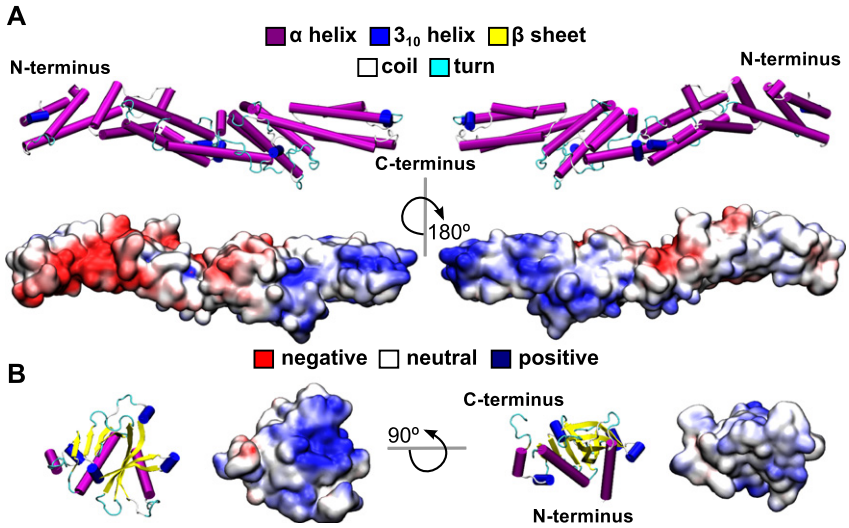

Fig. 1. Both Exo70p and Sec3p-N contain positively charged regions. A. The structure of Exo70p (PDB ID: 2PFV) and electrostatic potential mapped onto the solvent accessible surface calculated using the APBS program [70]. B. The structure of Sec3p-N (PDB ID: 3A58) and electrostatic potential mapped onto the solvent accessible surface. Electrostatic potential spans from −5 (red) to +5 (blue) kbT/e_c.

the whole structure could be divided into four domains (Fig. 1A). Despite the low sequence identity, all experimentally solved structures of exocyst subunits share the rod-like structural core composed of two or more consecutively packed helical bundles, with each bundle consisting of three to five α-helices linked by loops [16]. Analysis of the electrostatic potential mapped on the Exo70p surface revealed distinct polarity of the Exo70p structure [10,11] (Fig. 1A), where its N-terminal part is strongly negatively charged and the C-terminal part is positively charged. Interestingly, the prediction of the secondary structure suggests that the remaining unsolved exocyst subunits may be formed by similar helical folds [17]. In contrast to the rod-like structures described above, the crystal structure of N-terminal domain of Sec3p (Sec3p-N) revealed that this part folds into the Pleckstrin homology (PH)-like domain [13,14] (Fig. 1B). Sec3p-N (amino acid residues 76–260) is composed of three α-helices (α1–α3) and eight β-strands (β1–β8). The β1–β7 strands form an antiparallel β sheet resulting in the orthogonal sandwich and the abutting α2-helix typical for the PH-fold [14]. Examination of the electrostatic surface of Sec3p-N showed a positively charged pocket formed by three clusters of basic residues: i) R137 and R157, ii) R137, K135 and K155, and iii) R168 and K194 [14] (Fig. 1B).

A crucial aspect of the exocyst function is its tightly controlled interaction with PM. In the budding yeast cell, all exocyst subunits are polarized to the growing end of the daughter cell (bud tip), but the mechanisms of their targeting differ [16]. Although several alternative models have been proposed, Exo70p and Sec3p are generally believed to mediate the contact with the target PM region and thus ensure the specific localization of the whole complex. In most of the current models the remaining exocyst subunits are believed to be delivered to the exocytic sites with secretory vesicles on actin cables [18], but recent data indicate that in different organisms, dynamics of exocyst assembly and targeting may vary significantly [19,20]. A couple of recent reports showed that Sec3p and Exo70p interact with phosphatidylinositol (4,5)-bisphosphate (PIP_2), which is present predominantly in the inner leaflet of PM [21]. Sec3p binds PIP_2 via its N-terminal PH-like domain and basic residues located at the C-terminal part are important for Exo70p interaction with PIP_2 [13,14,21,22]. The disruption of the interaction of PIP_2 with both Sec3p and Exo70p inhibits PM-association of the exocyst and results in severe growth defects [21]. During the last 15 years, PIP_2 has emerged as an important second messenger especially in the regulation of cytoskeletal and membrane dynamics [23,24]. The distinctive features of PIP_2 are its bulky acidic headgroup, with the net charge ranging from −3 to −5 under physiological pH and an inverted conical overall shape that promotes positive curvature of membranes. PIP_2 functions by recruiting effector proteins to membranes in a spatio-temporally specific manner and/or it affects the biophysical properties of membranes.

To fully understand the exocyst function, it is important to explore the interaction of membrane-associating subunits of the exocyst and PIP_2 in the context of lipid bilayer. Molecular dynamics (MD) simulations have been shown to play an invaluable role in the molecular-level description of dynamic interaction of membrane proteins with phospholipids, which could be hardly obtained by experimental approaches [25,26]. In this study, we utilize coarse-grained MD simulations to reveal details of the specific Exo70p and Sec3p interaction with PIP_2. We also address simultaneous binding of Sec3p to PIP_2 and small GTPase Rho1p. Our results show an importance of the mutual interplay between PIP_2 molecules and proteins involved in exocytosis.

2. Methods

2.1. Structures used in the simulations

Before converting Exo70p structure (PDB ID: 2PFV, resolution of 2.10 Å, residues 67–623) [27] to the CG representation, the missing loop ILE224-PRO231 in the crystal structure was added using the program MODELLER 9.14 [28]. The structure of Sec3p-N was solved together with Rho1p (PDB ID: 3A58, resolution of 2.60 Å) [14] and both structures were used as a starting point for subsequent simulations. To convert exocyst subunits to the MARTINI v2.1 CG representation, we utilized the martinize.py script and we used the ELNEDYN representation with r_c = 0.9 nm and f_c = 500 kJ mol^{-1} nm^{-2} [29–31]. In the crystal structure of Sec3p-N-Rho1p, the C-terminal part of Rho1p called hypervariable region (HVR, amino acid residues 186 to 209) is missing, we therefore modeled this part as a random coil using the MODELLER 9.14 program. The ELNEDYN representation with r_c = 0.9 nm and f_c = 500 kJ mol^{-1} nm^{-2} was used to describe core of Rho1p and HVR was kept flexible. The C-terminal cysteine residue 207 of Rho1p was geranylgeranylated. The model of the geranylgeranyl tail consisted of a linear sequence of four C3 MARTINI beads, similarly to the published model of farnesyl moiety [32], all connected via harmonic bonds with r_0 = 0.49 nm and f_c = 8000 kJ mol^{-1} nm^{-2}. The angle bending was restricted by harmonic potentials with a = 140 equilibrium angle and f_c = 200 kJ mol^{-1}. The first C3 bead was connected to the cysteine side chain bead using a harmonic bond with r_0 = 0.39 nm and f_c = 5000 kJ mol^{-1} nm^{-2}.

2.2. Lipid bilayers

The MARTINI CG model for 1-palmitoyl-2-oleoylphosphatidylcholine (PC) was taken from [33] and 1-palmitoyl-2-oleoylphosphatidylinositol (4,5)-bisphosphate (PIP_2) molecule was prepared according to [34]. All lipid bilayers were generated by self-assembly CG-MD simulations. In these simulations, PC or PIP_2/PC lipids (without any protein) were randomly placed in a simulation box and solvated with coarse-grained water molecules and ions to neutralize the system. Then production simulations were performed for 500 ns. In all lipid bilayers, distribution of PIP_2 molecules in the leaflets was approximately equal (typically 4.5% vs. 4.9%). The membranes composed of 256 lipid molecules were subsequently used for the simulations with Sec3p-N and/or Rho1p. The lipid bilayers containing 1152 lipid molecules were used for the simulations of Exo70p.

2.3. Coarse-grained molecular dynamics simulations

The program GROMACS 4.5.0 was used for all MD simulations [35]. Lennard-Jones and electrostatic interactions were shifted to 0 between 9 and 12 Å and between 0 and 12 Å, respectively. A relative dielectric constant of 15 was used. Simulations were run in NPT ensemble. The temperature of protein, lipids, and solvent was coupled separately at 310 K using the Berendsen algorithm, with coupling constant 1.0 ps. The system pressure was coupled using the same algorithm with coupling constant 3.0 ps, compressibility of 3.0, and reference pressure of 1 bar. Simulations were performed using a 20 fs integration time step. Initially, protein was placed 2.5 nm apart the membrane prepared by the previous self-assembly simulation and dehydrated. Subsequently, we added standard MARTINI water and Na^+ ions to ensure electroneutrality of the system. We also performed simulation with polarizable MARTINI water model [36], in this case, we used MARTINI v2.2p for the protein description [31]. The whole system was energy minimized using steepest descent method up to maximum of 500 steps and production runs were performed for 1000 ns. It is important to note that times reported in this study are computational times. It was shown that effective times for CG simulations are longer; for proteins and lipids in MARTINI force field, the scaling factor is about four-fold [37], i.e. 1 μs simulation time would correspond to 4 μs real time. Standard Gromacs tools as well as in-house codes were used for analysis. The VMD program was used to prepare figures [38].

3. Results

3.1. Exo70p clusters PIP_2 molecules

To study the association of Exo70p with PIP_2-containing bilayer, we performed series of coarse-grained (CG)-MD simulations. Exo70p was initially placed ~2.5 nm from the center of mass of a lipid bilayer containing 5% PIP_2 and 95% phosphatidylcholine (PC, Fig. 2A). In all performed simulations (each of the 1 μs length), we observed binding of Exo70p to the lipid bilayer containing PIP_2. Exo70p diffused in the simulation box before associating with the lipid bilayer. An initial contact with the lipid bilayer was mediated by the C-terminal part of Exo70p; particularly amino acid residues K601, R604 and K605 started to interact with PIP_2 molecules (Fig. 2B). In four out of five simulations, a number of PIP_2 molecules interacting with the C-terminal part subsequently increased resulting in the association of the Exo70p domain D with the lipid bilayer (Fig. 2C). After 1 μs, the whole molecule of Exo70p associated with the lipid bilayer via several PIP_2-binding sites (Figs. 2D and 3). In these four simulations, the Exo70p interaction with the lipid bilayer containing PIP_2 was perfectly reproducible and stable. In the fifth simulation, Exo70p initially interacted with PIP_2 molecules by its C-terminus and it remained in this orientation for the subsequent simulation time (Fig. 2B). It is important to note, that the association of Exo70p with the lipid bilayer is PIP2-dependent, since we did not observe any interaction when a membrane was composed solely of PC (Fig. S1).

An analysis of the amino acid residues involved in the interaction of Exo70p with PIP_2 revealed that the highest number of interacting amino acid residues is located at the C-terminal part (Fig. 3A and B). These positively charged PIP_2-interacting sites located at Exo70p C-terminus correspond very well to the amino acids that were suggested to play a critical role in the PIP_2-binding by site-directed mutagenesis (in particular K538, K540, K567, K601 and K605) [21]. In addition to the C-terminal part, several other basic amino acid residues distributed along the membrane-associating surface of Exo70p contributed to the interaction with the PIP_2 molecules; particularly residues K168, K212, K228 and K489 (Fig. 3A and B).

A closer analysis of the Exo70p association with the lipid bilayer revealed that Exo70p clusters PIP_2 molecules in the adjacent leaflet of the lipid bilayer. This clustering could be visualized by employing average two-dimensional density of PIP_2 over the simulation length (Fig. 4). Local clusters of PIP_2 molecules are formed in the vicinity of the Exo70p (Fig. 4A). In contrast we did not observe any clustering in the opposite leaflet, which is not in contact with the protein (Fig. 4B). Hotspots of PIP_2 localization correspond to the identified binding sites on Exo70p. Notably, we observed fluctuations of individual PIP_2 molecules in the particular binding site, indicating that the simulated system reached equilibrium. We also performed simulations with the polarizable MARTINI force field [36]. In this case, we also observed that PIP_2 molecules specifically localize around Exo70p and thus these results further corroborate our hypothesis on the specific PIP_2 clustering mediated by Exo70p (Fig. S3).

We then asked whether membrane-associating surface of Exo70p is conserved through the evolution of eukaryotes. We constructed an alignment containing more than 150 Exo70 sequences covering various eukaryotic organisms (Supplementary Data 1) and we mapped the evolutionary conserved amino acid residues on the yeast Exo70p structure using Consurf algorithm [39]. We found that almost all amino acid

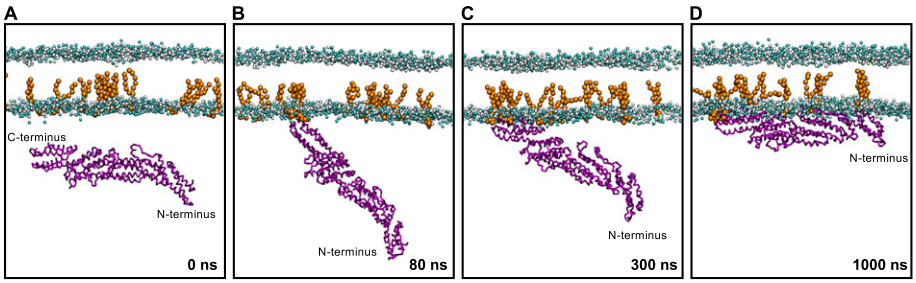

Fig. 2. Representative snapshots of the CG-MD simulation of Exo70p and membrane containing 5 % PIP_2 and 95% PC. The CG-MD simulation of Exo70p-membrane association shown at different simulating times, A 0 ns, B 80 ns, C 300 ns and D 1000 ns. CG water molecules and ions are not shown for the sake of clarity. Only PIP_2 molecules in the distance of 0.8 nm from the protein after 1000 ns are shown. Headgroup atoms of PC are shown in van der Waals representation (choline group in gray and phosphate group in light blue). Only protein backbone atoms are shown in licorice representation (purple).

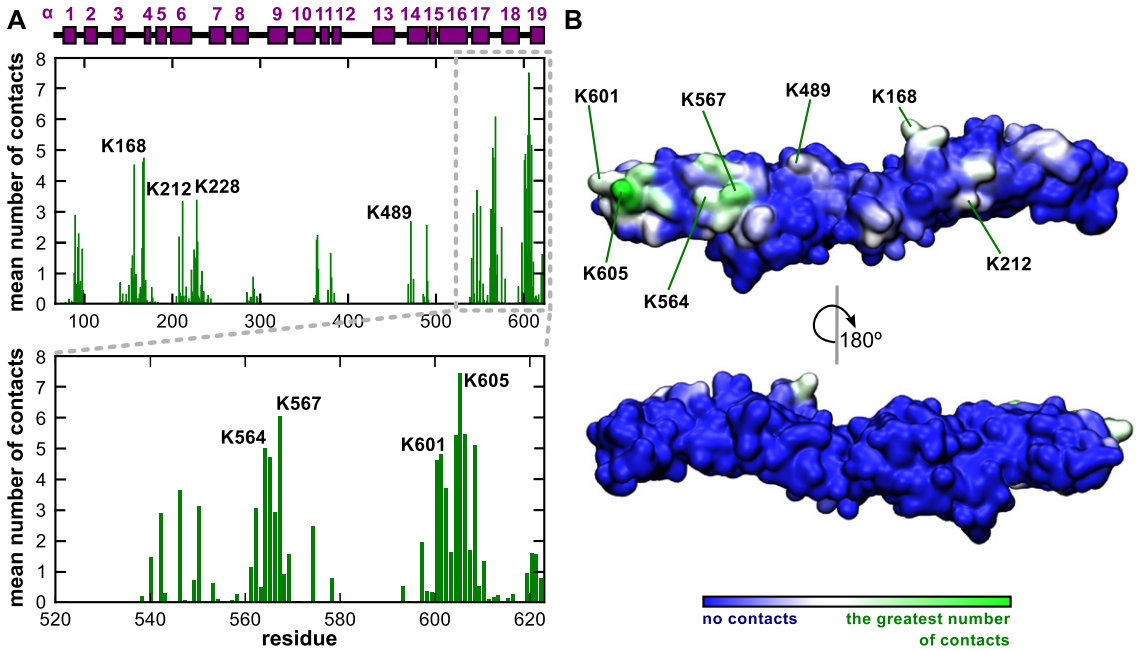

Fig. 3. Exo70p interacts with PIP_2 molecules by several amino acid residues distributed along the Exo70p structure. A. The mean number of Exo70p-PIP_2 contacts per residue. Contacts were defined as the number of PIP_2 phosphate groups within 0.8 nm of protein atoms. Contacts represent the average number computed from each performed simulation. B. Contacts mapped onto the Exo70p structure.

residues involved in the interaction with membrane are very well conserved (Fig. S2).

3.2. Sec3p-N interaction with PIP_2 is mediated by positively charged pocket

Having successfully revealed details of Exo70p-PIP_2 interaction, we then used the same approach to study dynamics of the Sec3p-N interaction with the lipid bilayer containing 5% PIP_2 and 95% PC. Initially, the protein was again placed ~2.5 nm from the center of mass of the lipid bilayer (Fig. 5A). In five performed simulations, Sec3p-N bound rapidly to the membrane, resulting in two orientations of Sec3p-N towards the membrane. In three simulations, the initial binding of PIP_2 molecules was mediated by amino acid residues R137, K155 and R157 (Fig. 5B). Subsequently, other residues started to interact with PIP_2 resulting in an equilibrated state, where the positively charged pocket of Sec3p-N coordinated several PIP_2 molecules (Fig. 5C). In this binding mode, the computed PIP_2-interacting residues are in perfect agreement with published experimental data (see below) [22]. Two other simulations ended in a reverse orientation of Sec3p-N towards the lipid bilayer and this orientation remained stable for additional 2 μs. We also performed simulations with the membrane composed solely from PC molecules and in this case, we observed no stable interaction of Sec3p-N with the lipid bilayer (Fig. S5).

In the binding mode, which is consistent with experimental results, PIP_2 molecules are coordinated by one positively charged pocket (residues K119, K135, R137, R157, R168 and K194; Fig. 6A and B). Our results are well supported by lipid-protein overlay analysis, which showed that combined mutations of these amino acid residues abrogate the PIP_2 binding *in vitro* [14]. In addition to these six residues, K100 located at the very end of the α1-helix contributed to the PIP_2 binding. Intriguingly, this residue was also able to form non-specific polar contact with phosphate atoms of PC when lower concentration of PIP_2 was used

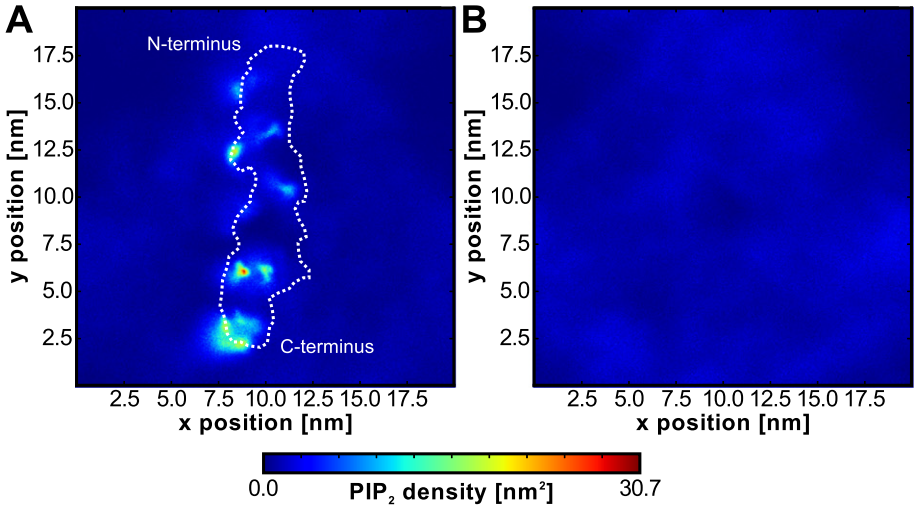

Fig. 4. Exo70p mediates PIP_2 clustering. A. The typical example of two-dimensional density of PIP_2 molecules in the leaflet adjacent to Exo70p calculated over last 500 ns of the simulation. B. The typical example of two-dimensional density of PIP_2 molecules in the leaflet, which is not in contact with Exo70p calculated over last 500 ns of the simulation.

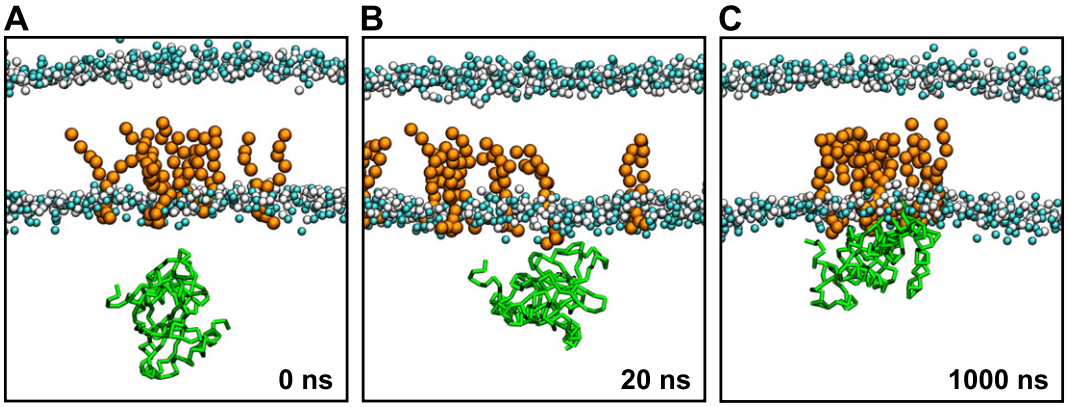

Fig. 5. Representative snapshots from the CG-MD simulation of Sec3p and membrane containing PIP_2. The CG-MD simulation of Sec3p-N-membrane association shown at different simulating times, A 0 ns, B 20 ns and C 1000 ns. CG water molecules and ions are not shown for the sake of clarity. Only PIP_2 molecules in the distance of 0.8 nm from the protein after 1000 ns are shown. Headgroup atoms of PC are shown in van der Waals representation (choline group in gray and phosphate group in light blue). Only protein backbone atoms are shown in licorice representation (green).

(data not shown). It is important to mention, that the observation of Sec3p-N orientation towards the membrane, which is not supported by experimental results, could be an artifact of CG-model. Other explanation could be that in our model, a large fraction of Sec3p molecule is unavailable or other factors have to be taken into account (e.g. Rho1p, see below).

Similarly to Exo70p, we performed analysis of conserved amino acid residues through various eukaryotes. Also in the case of Sec3p-N, the membrane-interacting residues are very well conserved through the evolution (Fig. S5, Supplementary Data 2).

3.3. Sec3p-N interacts simultaneously with Rho1p and membrane containing PIP_2

CG-MD simulations have been successfully used to describe complex systems containing the lipid bilayer and more than a single protein, e.g. it helped to probe the mechanism of the integrin inside-out activation [40]. To explore specificity of the Sec3p-N targeting, we took advantage of this capability of CG-MD and of the fact, that Sec3p-N was co-crystallized together with small GTPase Rho1p in the active state [14]. Rho1p is a member of the Rho family of small GTP-binding proteins, which are master regulators of many cellular activities [41]. It is a peripheral membrane protein, which is anchored to the lipid bilayer via geranylgeranyl moiety posttranslationally added at its C-terminal region. As the highly flexible C-terminal region (also called the hypervariable region — HVR, corresponding to amino acid residues 186 to 209) is missing in the available crystal structure of Rho1p, we modeled it using the MODELLER program [28]. A similar strategy was shown to give results in a very good agreement with experiments for other small GTPase [32,42,43].

We first simulated the interaction of Rho1p with the lipid bilayer composed solely of PC. Three independent simulations converged into a single orientation of Rho1p towards the membrane (Fig. 7A). This almost parallel orientation of Rho1p to the plane of the lipid bilayer is in a very good agreement with previously published results for other small GTPases, namely H-Ras and Rheb [42,44]. It was shown that during cytokinesis, Rho1p targeting to PM is dependent on PIP_2. Moreover Rho1p HVR can directly interact with phosphoinositides via a stretch of positively charged residues [45]. Therefore, we further performed simulations with Rho1p alone anchored to the lipid bilayer composed of 5% PIP_2 and 95% PC. In an equilibrated state, PIP_2 molecules are preferentially bound to lysine residues located at HVR (Fig. S7). When PIP_2 is present in the lipid bilayer, the Rho1p orientation towards the plane of the lipid bilayer is much more perpendicular than if only PC is present (Fig. 7B and C). Also, when PIP_2 molecules were replaced by PC molecules in the equilibrated system, Rho1p adopted the same orientation towards the membrane as in the simulation with PC only membrane. These results showed the effect of PIP_2 on the positioning of Rho1p and we hypothesize that this effect could have an important impact on further interactions of Rho1p with other proteins.

It was suggested that Sec3p-N is able to simultaneously bind both the small GTPase and phosphoinositides [14]. To test this hypothesis, we used the last snapshot from the simulation of Rho1p with the membrane containing PIP_2 and we added Sec3p-N (Fig. 8). We observed

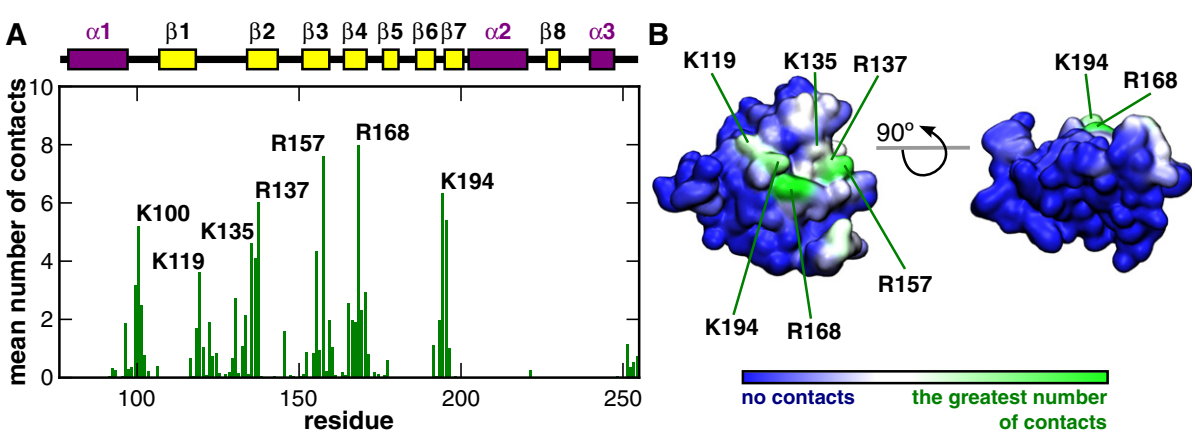

Fig. 6. Sec3p-N coordinates PIP_2 molecules by the positively charged pocket. A. The mean number of Sec3p-N-PIP_2 contacts per residue. Contacts were defined as the number of PIP_2 phosphate groups within 0.8 nm of protein atoms. Contacts represent the average number computed from each performed simulation. B. Contacts mapped onto the Sec3p-N structure.

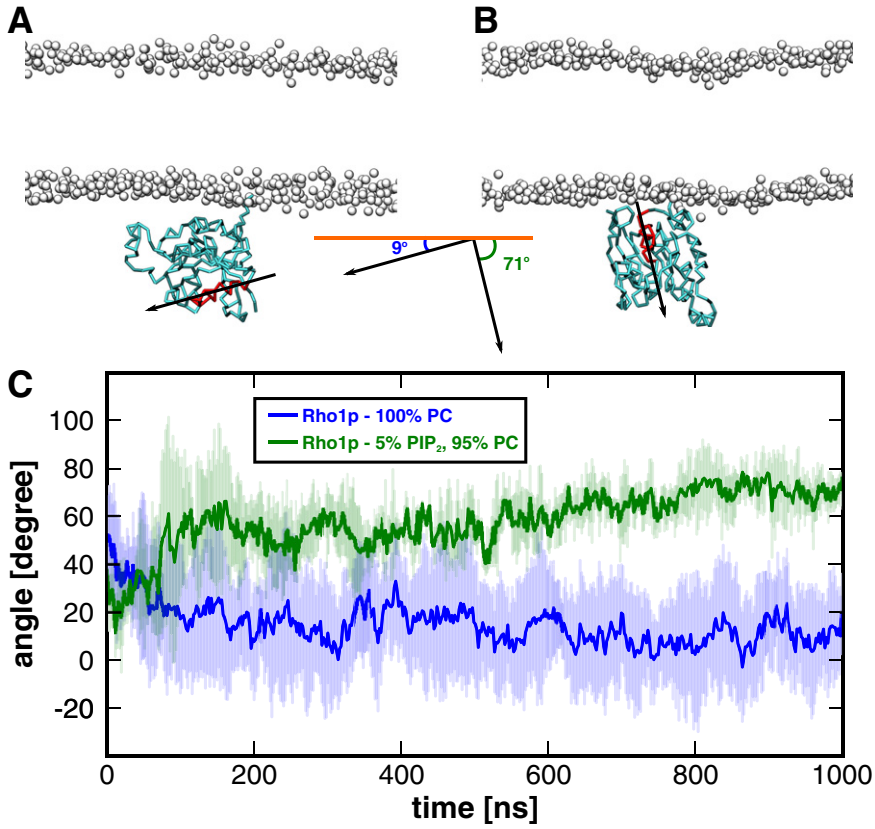

Fig. 7. The effect of PIP_2 on the Rho1p interaction with membrane. A. The final snapshot of CG-MD simulation of Rho1p association with membrane composed from PC. B. The final snapshot of CG-MD simulation of Rho1p association with membrane containing 5% PIP_2 (not shown for the sake of clarity). Numbers in A and B are values of angles between axes defined by α helix 6 of Rho1p (highlighted in red) and Z-axis. C. Time-evolution of the angle between Rho1p α 6 helix and Z-axis.

formation of a stable dimer between Sec3p-N and Rho1p in all five simulations (Fig. 8B and C). Importantly, both Sec3p-N and Rho1p proteins still interacted with the lipid bilayer at the same time.

We compared amino acid residues involved in the interaction between Sec3p-N and Rho1p in the presence of the membrane with control simulations starting from the published crystal structure without a lipid bilayer (HVR of Rho1p was excluded), and we found an almost perfect agreement (Fig. 9). As originally described, most contacts between Rho1p and Sec3p-N are hydrophobic (Fig. S6) [14]. In the case of Sec3p-N, we were able to correctly reproduce all contacts with Rho1p (Fig. 9A). An analysis of Rho1p amino acid residues interacting with Sec3p revealed that most contacts are well reproduced in our simulations with the lipid bilayer, but we obtained an additional patch of amino acid residues (around F111), which is not present in the control simulation. However, it is important to note, that calculated contacts in this patch show a large statistical uncertainty. Interestingly, when we calculated contacts of Sec3p-N and Rho1p with PIP_2 molecules, we found almost no overlap with residues involved in the protein–protein interaction, further supporting the existence of the functional Sec3p-Rho1p complex bound to the membrane (Fig. 9).

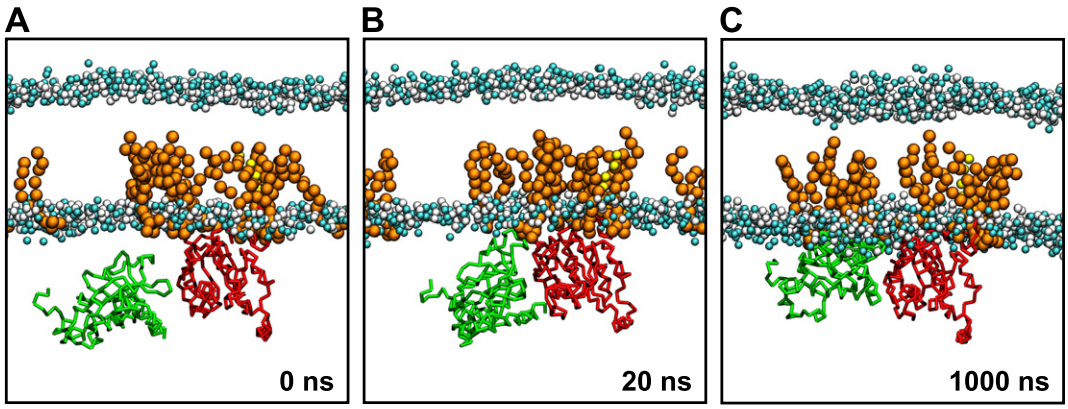

Fig. 8. Representative snapshots from CG-MD simulation of Sec3p-N-Rho1p interaction shown at different simulating times, A 0 ns, B 20 ns and C 1000 ns. CG water molecules and ions are not shown for the sake of clarity. Only PIP_2 molecules in the distance of 0.8 nm from the proteins after 1000 ns are shown. Headgroup atoms of PC are shown in van der Waals representation (choline group in gray and phosphate group in light blue). Only protein backbone atoms are shown in licorice representation (Sec3p-N is in green and Rho1p is in red).

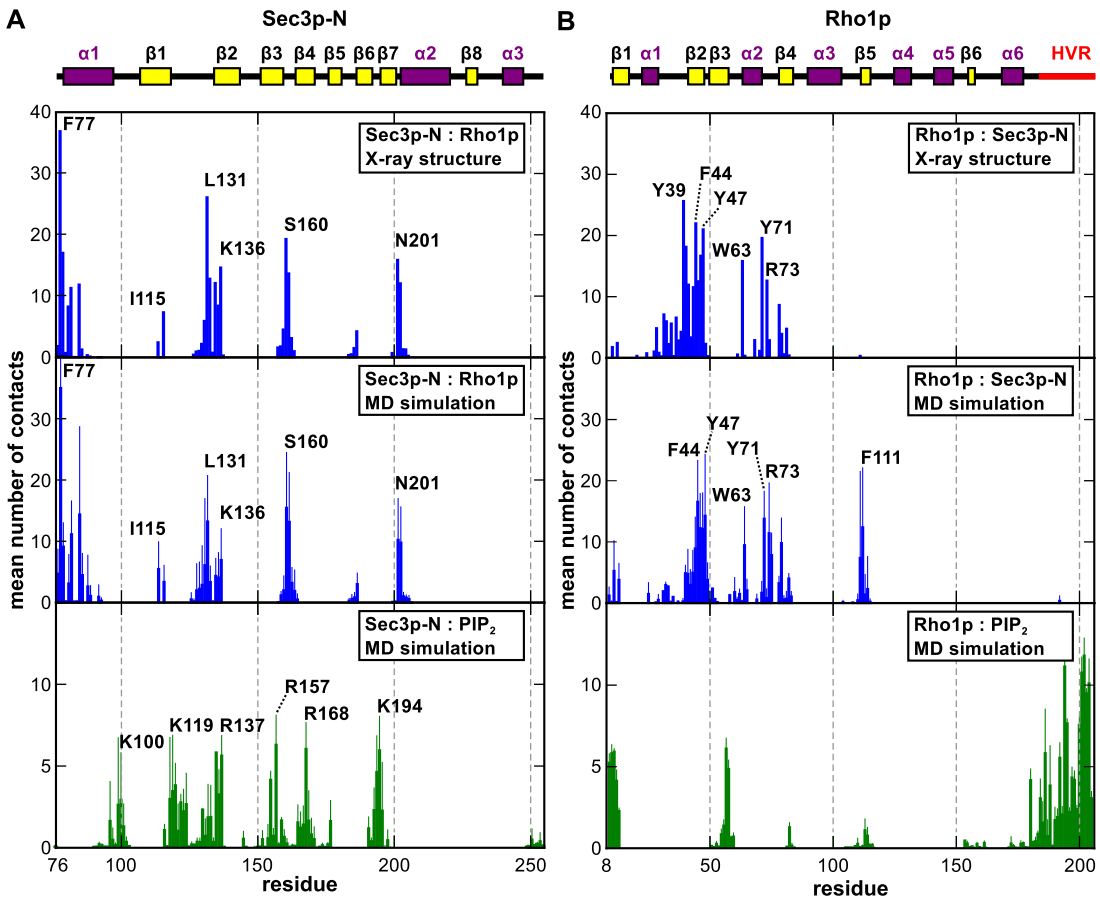

Fig. 9. Amino acid residues involved in the interaction between Sec3p-N and Rho1p. A. The comparison of Sec3p-N amino acid residue interacting with Rho1p. B. The comparison of Sec3p-N amino acid residue interacting with Rho1p. Upper panels represent protein–protein contacts calculated for simulations started from the crystal structure (PDB ID: 3A58), middle panels contain protein–protein contacts calculated for simulations describing the formation of Sec3p-N:Rho1p dimer in PIP2-containing lipid bilayer. Bottom panels show amino acid residues involved in the interaction with PIP_2 molecules. The average numbers of contacts with standard errors computed from five simulations over last 500 ns are shown.

4. Discussion and conclusions

Exocytosis is one of the most fundamental processes in eukaryotic cells. It is crucial for cell expansion, cell division and also for intercellular signaling between cells. During the last two decades, many components of exocytotic machinery have been discovered. By its nature, exocytosis is a process at the boundary between cytoplasm and PM, but we still know surprisingly little about the molecular details and especially the dynamic of interactions between proteins and lipids involved. Since the exocyst is required for both determining the site of fusion of secretory vesicles with the plasma membrane and, at the same time, for mechanistic tethering of secretory vesicles to PM, we focused on the interaction of the membrane-associating subunits of the exocyst complex, Exo70p and Sec3p with PIP_2 signaling phospholipids.

Using CG-MD simulations, we identified several PIP_2-binding sites distributed along the yeast Exo70p structure with the greatest number of interacting amino acid residues located at the Exo70p C-terminus (Fig. 3). Strikingly, the Exo70p association with the lipid bilayer containing PIP_2 resembles the interaction mode of BAR domains [46]. It was shown that Exo70p could act in a similar fashion as the BAR domain in promoting membrane curvature [47]. Our data showed that Exo70p induces the formation of PIP_2 clusters (Fig. 4). Interestingly, several recent papers described the same behavior for BAR domains experimentally [48,49]. PIP_2 has been implicated in the priming and mediating of exocytosis; it localizes to the exocytic sites and it recruits and modulates the activity of several proteins involved in SNARE-mediated vesicle fusion [50]. Several possible mechanisms, which are not mutually exclusive, have been described to mediate formation of PIP_2 clusters. It is believed that PIP_2 molecules align with cholesterol-rich regions in the cytoplasmic leaflet of PM, although there is still some controversy about the effect of cholesterol [51]. Ca^{2+} ions were clearly shown to form bridges between individual PIP_2 molecules resulting in the PIP_2-enriched fractions [52]. Other described factors mediating PIP_2 clustering are proteins, e.g. highly positively charged MARCK peptides interact with anionic PIP_2 headgroups and sequester PIP_2 molecules to the clusters [53]. Based on our results, we hypothesize that Exo70p could act in a similar manner and it could contribute to form patches of the high local PIP_2 concentration, thus resulting in exocytic hotspots. It has been shown that protein–protein interactions in aqueous solution are overrepresented with the standard MARTINI force field [54]. Nevertheless, results from analogous simulations of protein–lipid interactions seem to reproduce experimental results very well [26,55–60]. We therefore believe that observed PIP_2 clustering is not simply artifact of the CG model.

In yeast, the PIP_2 distribution in PM is rather widespread and not restricted to the forming daughter cell membrane (i.e. the site of extensive secretion) and therefore other factors contributing to the polarized localization of the exocyst must exist [16]. Small GTP-binding proteins from the Rho family were described as important polarity determinants [41]. Indeed, it was documented that Exo70p binds Rho3p and Sec3p-N directly interacts with Rho1p and Cdc42p members of the Rho GTPase family [14,41,61–64]. It was, therefore, hypothesized that small GTPases together with PIP_2 could control the exocyst localization at the different cell cycle stages or growth conditions [16]. Our new findings well support this.

In this work, we investigated the effect of PIP_2 on the interaction of Sec3p-N with Rho1p in the context of a lipid bilayer. We found a strong effect of PIP_2 on the orientation of the Rho1p core towards membrane (Fig. 7). Importantly, Sec3p-N can interact simultaneously with Rho1p and PIP_2 only when Rho1p adopts the active (PIP_2-mediated) conformation (Fig. 8). We therefore speculate that a vivid interplay between Rho1p and PIP_2 determines localization of Sec3 exocyst subunit. It is also important to mention that the stable polarization of Sec3p and Exo70p also depends on the other subunits of the exocyst complex [65–67], but molecular details on the exocyst assembly and recycling remain to be elucidated.

The analysis of conserved amino acid residues showed that membrane-interacting regions of both Exo70p and Sec3p-N are well conserved throughout eukaryotic sequences (Figs. S2 and S5). Recently, Bem1p was described as a factor contributing to the Exo70p localization [68]. It was shown that Bem1p directly binds Exo70p and amino acid residues involved in the interaction were determined. Interestingly, those amino acid residues are very variable among eukaryotic Exo70s (Fig. S7). The same is true for amino acid residues involved in the Exo70p binding of Rho3p (data not shown). Similarly, amino acid residues involved in the interaction of Sec3p-N with Rho1p are also not conserved in eukaryotic sequences (Fig. S8). Moreover, mammalian Exo70 is phosphorylated at amino acid residue serine 250, which is involved in the interaction with the other subunits [69], but this residue is not conserved outside Deuterostomia. Taken together our results strongly suggest that membrane-association of the exocyst subunits conveyed through minor acidic phospholipids is evolutionarily conserved and probably represents an ancestral mechanism of exocyst targeting. On the other hand, the control of exocyst function through protein–protein interactions of individual subunits with other regulatory proteins is rather organism specific. Given the availability of structural data for other related tethering CATCHR complexes involved in endomembrane trafficking (such as Dsl, COG, GARP) [8], our study also calls for thorough future investigations of possible shared mechanism of these protein complexes interactions with their target membranes.

Supplementary data to this article can be found online at http://dx.doi.org/10.1016/j.bbamem.2015.03.026.

Transparency document

The transparency document associated with this article can be found, in the online version.

Acknowledgements

This work was supported by the Czech Grant Agency grant GACR 13-19073S to M.P. P. J. acknowledges support from the Czech Grant Agency (grant no. P208/12/G016) and via the Praemium Academiae Award. A part of V.Ž. income is covered by MŠMT ČR project NPUI LO1417. The authors thank Dr. Lukáš Synek (IEB Prague, Czech Republic) for critical reading of the manuscript. The authors express their thanks to the developers of Linux operation system and open-source programs used in preparation of this study, particularly Gimp, Gnumeric, Gromacs, Inkscape, VMD and Zotero.

References

[1] M.R. Heider, M. Munson, Exorcising the exocyst complex, Traffic 13 (2012) 898–907.
[2] M. Hertzog, P. Chavrier, Cell polarity during motile processes: keeping on track with the exocyst complex, Biochem. J. 433 (2011) 403–409.
[3] V. Žárský, I. Kulich, M. Fendrych, T. Pečenková, Exocyst complexes multiple functions in plant cells secretory pathways, Curr. Opin. Plant Biol. 16 (2013) 726–733.
[4] K. Orlando, W. Guo, Membrane organization and dynamics in cell polarity, Cold Spring Harb. Perspect. Biol. 1 (2009) a001321.
[5] H. Cai, K. Reinisch, S. Ferro-Novick, Coats, tethers, Rabs, and SNAREs work together to mediate the intracellular destination of a transport vesicle, Dev. Cell 12 (2007) 671–682.
[6] P. Novick, C. Field, R. Schekman, Identification of 23 complementation groups required for post-translational events in the yeast secretory pathway, Cell 21 (1980) 205–215.
[7] D.R. TerBush, T. Maurice, D. Roth, P. Novick, The exocyst is a multiprotein complex required for exocytosis in *Saccharomyces cerevisiae*, EMBO J. 15 (1996) 6483–6494.
[8] W. Hong, S. Lev, Tethering the assembly of SNARE complexes, Trends Cell Biol. 24 (2014) 35–43.
[9] J. Liu, W. Guo, The exocyst complex in exocytosis and cell migration, Protoplasma 249 (2012) 587–597.
[10] G. Dong, A.H. Hutagalung, C. Fu, P. Novick, K.M. Reinisch, The structures of exocyst subunit Exo70p and the Exo84p C-terminal domains reveal a common motif, Nat. Struct. Mol. Biol. 12 (2005) 1094–1100.
[11] Z.A. Hamburger, A.E. Hamburger, A.P. West Jr., W.I. Weis, Crystal structure of the *S cerevisiae* exocyst component Exo70p, J. Mol. Biol. 356 (2006) 9–21.
[12] M.V.S. Sivaram, M.L.M. Furgason, D.N. Brewer, M. Munson, The structure of the exocyst subunit Sec6p defines a conserved architecture with diverse roles, Nat. Struct. Mol. Biol. 13 (2006) 555–556.
[13] K. Baek, A. Knödler, S.H. Lee, X. Zhang, K. Orlando, J. Zhang, T.J. Foskett, W. Guo, R. Dominguez, Structure–function study of the N-terminal domain of exocyst subunit Sec3, J. Biol. Chem. 285 (2010) 10424–10433.
[14] M. Yamashita, K. Kurokawa, Y. Sato, A. Yamagata, H. Mimura, A. Yoshikawa, K. Sato, A. Nakano, S. Fukai, Structural basis for the Rho- and phosphoinositide-dependent localization of the exocyst subunit Sec3, Nat. Struct. Mol. Biol. 17 (2010) 180–186.
[15] S. Wu, S.Q. Mehta, F. Pichaud, H.J. Bellen, F.A. Quiocho, Sec15 interacts with Rab11 via a novel domain and affects Rab11 localization in vivo, Nat. Struct. Mol. Biol. 12 (2005) 879–885.
[16] B. He, W. Guo, The exocyst complex in polarized exocytosis, Curr. Opin. Cell Biol. 21 (2009) 537–542.
[17] N.J. Croteau, M.L.M. Furgason, D. Devos, M. Munson, Conservation of helical bundle structure between the exocyst subunits, PLoS One 4 (2009) e4443.
[18] C. Boyd, T. Hughes, M. Pypaert, P. Novick, Vesicles carry most exocyst subunits to exocytic sites marked by the remaining two subunits, Sec3p and Exo70p, J. Cell Biol. 167 (2004) 889–901.
[19] M. Fendrych, L. Synek, T. Pečenková, E.J. Drdová, J. Sekereš, R. de Rycke, M.K. Nowack, V. Žárský, Visualization of the exocyst complex dynamics at the plasma membrane of *Arabidopsis thaliana*, Mol. Biol. Cell 24 (2013) 510–520.
[20] M. Riquelme, E.L. Bredeweg, O. Callejas-Negrete, R.W. Roberson, S. Ludwig, A. Beltrán-Aguilar, S. Seiler, P. Novick, M. Freitag, The *Neurospora crassa* exocyst complex tethers Spitzenkörper vesicles to the apical plasma membrane during polarized growth, Mol. Biol. Cell 25 (2014) 1312–1326.
[21] B. He, F. Xi, X. Zhang, J. Zhang, W. Guo, Exo70 interacts with phospholipids and mediates the targeting of the exocyst to the plasma membrane, EMBO J. 26 (2007) 4053–4065.
[22] X. Zhang, K. Orlando, B. He, F. Xi, J. Zhang, A. Zajac, W. Guo, Membrane association and functional regulation of Sec3 by phospholipids and Cdc42, J. Cell Biol. 180 (2008) 145–158.
[23] P.A. Janmey, U. Lindberg, Cytoskeletal regulation: rich in lipids, Nat. Rev. Mol. Cell Biol. 5 (2004) 658–666.
[24] R. Pleskot, P. Pejchar, C.J. Staiger, M. Potocký, When fat is not bad: the regulation of actin dynamics by phospholipid signaling molecules, Front. Plant Sci. 5 (2014) 5.
[25] S.J. Marrink, A.H. de Vries, D.P. Tieleman, Lipids on the move: simulations of membrane pores, domains, stalks and curves, Biochim. Biophys. Acta Biomembr. 1788 (2009) 149–168.
[26] P.J. Stansfeld, M.S.P. Sansom, Molecular simulation approaches to membrane proteins, Structure 19 (2011) 1562–1572.
[27] B.A. Moore, H.H. Robinson, Z. Xu, The crystal structure of mouse Exo70 reveals unique features of the mammalian exocyst, J. Mol. Biol. 371 (2007) 410–421.
[28] A. Šali, T.L. Blundell, Comparative protein modelling by satisfaction of spatial restraints, J. Mol. Biol. 234 (1993) 779–815.
[29] L. Monticelli, S.K. Kandasamy, X. Periole, R.G. Larson, D.P. Tieleman, S.J. Marrink, The MARTINI coarse-grained force field: extension to proteins, J. Chem. Theory Comput. 4 (5) (2008) 819–834.
[30] X. Periole, M. Cavalli, S.-J. Marrink, M.A. Ceruso, Combining an elastic network with a coarse-grained molecular force field: structure, dynamics, and intermolecular recognition, J. Chem. Theory Comput. 5 (2009) 2531–2543.
[31] D.H. de Jong, G. Singh, W.F.D. Bennett, C. Arnarez, T.A. Wassenaar, L.V. Schäfer, X. Periole, D.P. Tieleman, S.J. Marrink, Improved parameters for the Martini coarse-grained protein force field, J. Chem. Theory Comput. 9 (2012) 687–697.
[32] D.H. de Jong, C.A. Lopez, S.J. Marrink, Molecular view on protein sorting into liquid-ordered membrane domains mediated by gangliosides and lipid anchors, Faraday Discuss. 161 (2013) 347–363.
[33] S.J. Marrink, H.J. Risselada, S. Yefimov, D.P. Tieleman, A.H. de Vries, The MARTINI force field: coarse grained model for biomolecular simulations, J. Phys. Chem. B 111 (2007) 7812–7824.
[34] P.J. Stansfeld, R. Hopkinson, F.M. Ashcroft, M.S.P. Sansom, PIP2-binding site in Kir channels: definition by multiscale biomolecular simulations, Biochemistry (Mosc) 48 (2009) 10926–10933.
[35] B. Hess, C. Kutzner, D. van der Spoel, E. Lindahl, GROMACS 4: algorithms for highly efficient, load-balanced, and scalable molecular simulation, J. Chem. Theory Comput. 4 (2008) 435–447.
[36] S.O. Yesylevskyy, L.V. Schäfer, D. Sengupta, S.J. Marrink, Polarizable water model for the coarse-grained MARTINI force field, PLoS Comput. Biol. 6 (2010) e1000810.
[37] S.J. Marrink, D.P. Tieleman, Perspective on the Martini model, Chem. Soc. Rev. 42 (2013) 6801.
[38] W. Humphrey, A. Dalke, K. Schulten, VMD: visual molecular dynamics, J. Mol. Graph. 14 (1996) 33–38.

[39] H. Ashkenazy, E. Erez, E. Martz, T. Pupko, N. Ben-Tal, ConSurf 2010: calculating evolutionary conservation in sequence and structure of proteins and nucleic acids, Nucleic Acids Res. 38 (2010) W529–W533.
[40] A.C. Kalli, I.D. Campbell, M.S.P. Sansom, Multiscale simulations suggest a mechanism for integrin inside-out activation, Proc. Natl. Acad. Sci. 108 (2011) 11890–11895.
[41] W. Guo, F. Tamanoi, P. Novick, Spatial regulation of the exocyst complex by Rho1 GTPase, Nat. Cell Biol. 3 (2001) 353–360.
[42] A.A. Gorfe, M. Hanzal-Bayer, D. Abankwa, J.F. Hancock, J.A. McCammon, Structure and dynamics of the full-length lipid-modified H-Ras protein in a 1,2-dimyristoylglycero-3-phosphocholine bilayer, J. Med. Chem. 50 (2007) 674–684.
[43] E. Jefferys, M.S.P. Sansom, P.W. Fowler, NRas slows the rate at which a model lipid bilayer phase separates, Faraday Discuss. 169 (2014) 209–223.
[44] M.T. Mazhab-Jafari, C.B. Marshall, P.B. Stathopulos, Y. Kobashigawa, V. Stambolic, L.E. Kay, F. Inagaki, M. Ikura, Membrane-dependent modulation of the mTOR activator Rheb: NMR observations of a GTPase tethered to a lipid-bilayer nanodisc, J. Am. Chem. Soc. 135 (2013) 3367–3370.
[45] S. Yoshida, S. Bartolini, D. Pellman, Mechanisms for concentrating Rho1 during cytokinesis, Genes Dev. 23 (2009) 810–823.
[46] B. Qualmann, D. Koch, M.M. Kessels, Let's go bananas: revisiting the endocytic BAR code, EMBO J. 30 (2011) 3501–3515.
[47] Y. Zhao, J. Liu, C. Yang, B.R. Capraro, T. Baumgart, R.P. Bradley, N. Ramakrishnan, X. Xu, R. Radhakrishnan, T. Svitkina, W. Guo, Exo70 generates membrane curvature for morphogenesis and cell migration, Dev. Cell 26 (2013) 266–278.
[48] J. Saarikangas, H. Zhao, A. Pykäläinen, P. Laurinmäki, P.K. Mattila, P.K.J. Kinnunen, S.J. Butcher, P. Lappalainen, Molecular mechanisms of membrane deformation by I-BAR domain proteins, Curr. Biol. 19 (2009) 95–107.
[49] H. Zhao, A. Michelot, E.V. Koskela, V. Tkach, D. Stamou, D.G. Drubin, P. Lappalainen, Membrane-sculpting BAR domains generate stable lipid microdomains, Cell Rep. 4 (2013) 1213–1223.
[50] T.F.J. Martin, PI(4,5)P2-binding effector proteins for vesicle exocytosis, Biochim. Biophys. Acta (BBA) - Mol. Cell Biol. Lipids 1851 (2015) 785–793.
[51] Y.-H. Wang, D.R. Slochower, P.A. Janmey, Counterion-mediated cluster formation by polyphosphoinositides, Chem. Phys. Lipids 182 (2014) 38–51.
[52] Y.-H. Wang, A. Collins, L. Guo, K.B. Smith-Dupont, F. Gai, T. Svitkina, P.A. Janmey, Divalent cation-induced cluster formation by polyphosphoinositides in model membranes, J. Am. Chem. Soc. 134 (2012) 3387–3395.
[53] S. McLaughlin, D. Murray, Plasma membrane phosphoinositide organization by protein electrostatics, Nature 438 (2005) 605–611.
[54] A.C. Stark, C.T. Andrews, A.H. Elcock, Toward optimized potential functions for protein–protein interactions in aqueous solutions: osmotic second virial coefficient calculations using the MARTINI coarse-grained force field, J. Chem. Theory Comput. 9 (2013) 4176–4185.
[55] R. Pleskot, P. Pejchar, V. Žárský, C.J. Staiger, M. Potocký, Structural insights into the inhibition of actin-capping protein by interactions with phosphatidic acid and phosphatidylinositol (4,5)-bisphosphate, PLoS Comput. Biol. 8 (2012) e1002765.
[56] C.N. Lumb, M.S.P. Sansom, Finding a needle in a haystack: the role of electrostatics in target lipid recognition by PH domains, PLoS Comput. Biol. 8 (2012) e1002617.
[57] C. Arnarez, S.J. Marrink, X. Periole, Identification of cardiolipin binding sites on cytochrome c oxidase at the entrance of proton channels, Sci. Rep. 3 (2013).
[58] C. Arnarez, J.-P. Mazat, J. Elezgaray, S.-J. Marrink, X. Periole, Evidence for cardiolipin binding sites on the membrane-exposed surface of the cytochrome bc1, J. Am. Chem. Soc. 135 (2013) 3112–3120.
[59] M.R. Schmidt, P.J. Stansfeld, S.J. Tucker, M.S.P. Sansom, Simulation-based prediction of phosphatidylinositol 4,5-bisphosphate binding to an ion channel, Biochemistry (Mosc) 52 (2013) 279–281.
[60] M. Weingarth, A. Prokofyev, E.A.W. van der Cruijsen, D. Nand, A.M.J.J. Bonvin, O. Pongs, M. Baldus, Structural determinants of specific lipid binding to potassium channels, J. Am. Chem. Soc. 135 (2013) 3983–3988.
[61] J.E. Adamo, G. Rossi, P. Brennwald, The Rho GTPase Rho3 has a direct role in exocytosis that is distinct from its role in actin polarity, Mol. Biol. Cell 10 (1999) 4121–4133.
[62] N.G.G. Robinson, L. Guo, J. Imai, A. Toh-e, Y. Matsui, F. Tamanoi, Rho3 of *Saccharomyces cerevisiae*, which regulates the actin cytoskeleton and exocytosis, is a GTPase which interacts with Myo2 and Exo70, Mol. Cell. Biol. 19 (1999) 3580–3587.
[63] X. Zhang, E. Bi, P. Novick, L. Du, K.G. Kozminski, J.H. Lipschutz, W. Guo, Cdc42 interacts with the exocyst and regulates polarized secretion, J. Biol. Chem. 276 (2001) 46745–46750.
[64] H. Wu, C. Turner, J. Gardner, B. Temple, P. Brennwald, The Exo70 subunit of the exocyst is an effector for both Cdc42 and Rho3 function in polarized exocytosis, Mol. Biol. Cell 21 (2010) 430–442.
[65] O. Roumanie, H. Wu, J.N. Molk, G. Rossi, K. Bloom, P. Brennwald, Rho GTPase regulation of exocytosis in yeast is independent of GTP hydrolysis and polarization of the exocyst complex, J. Cell Biol. 170 (2005) 583–594.
[66] X. Zhang, A. Zajac, J. Zhang, P. Wang, M. Li, J. Murray, D. TerBush, W. Guo, The critical role of Exo84p in the organization and polarized localization of the exocyst complex, J. Biol. Chem. 280 (2005) 20356–20364.
[67] J.A. Songer, M. Munson, Sec6p anchors the assembled exocyst complex at sites of secretion, Mol. Biol. Cell 20 (2009) 973–982.
[68] D. Liu, P. Novick, Bem1p contributes to secretory pathway polarization through a direct interaction with Exo70p, J. Cell Biol. 207 (2014) 59–72.
[69] J. Ren, W. Guo, ERK1/2 regulate exocytosis through direct phosphorylation of the exocyst component Exo70, Dev. Cell 22 (2012) 967–978.
[70] N.A. Baker, D. Sept, S. Joseph, M.J. Holst, J.A. McCammon, Electrostatics of nanosystems: application to microtubules and the ribosome, Proc. Natl. Acad. Sci. 98 (2001) 10037–10041.